Development of a proposed design method for discontinuous columns in braced frames

C.M. King[a,b] and J.B. Davison[c]

[a] *Steel Construction Institute, Silwood Park, Ascot, Berkshire, SL5 7QN, UK*
[b] *COWI North America, 101-788 Harbourside Drive, North Vancouver, BC, Canada V7P 3R7*
[c] *Department of Civil and Structural Engineering, University of Sheffield, Sheffield S1 3JD, UK*
 Corresponding author - j.davison@sheffield.ac.uk T: +44(0)114 2225354 F: +44(0)114 2225700

Abstract

A column design method has been developed for use in braced frames with discontinuous columns using flexible cap and base plates and floor beams that are either simply supported or continuous. The proposed method is intended to be used with shallow floor construction with concrete or steel/concrete composite slabs in which the floor slab occupies the depth of the floor beams and is fully grouted to the beams so that the slab restrains the full depth of the beams. It was developed to simplify the design of square hollow sections discontinuous columns in frames using asymmetric beam (ASB) type floor construction. Floor beams are designed to carry the floor loads without interaction with the columns; columns are then designed to resist the floor beam reactions assuming a deformed shape derived from end-rotations equal to the slope of the floor beams at the top or bottom of the column, whichever is the greater. The method incorporates the elasto-plastic behaviour of columns subject to axial compression and large end-rotations and has been verified by physical tests on full-scale square hollow sections columns and finite element analysis using non-linear geometry and material properties and including residual stresses.

Keywords: column design; discontinuous columns; moment shedding; plasticity; tubular steel

2 Introduction

In braced steel frame construction it is usual practice for a single length of column to extend over two or more stories and for the beams to frame into the continuous column and be connected by connections designed for vertical shear. Recently a new form of braced frame has been used in the UK for residential construction in which the columns are discontinuous [1]. Columns are fabricated in single storey lengths and fitted with horizontal plates (known as cap- or end- plates) at the top and bottom in order to bolt the column directly to beams below and above which are continuous over the column. Square hollow sections with the smallest possible size are used for the columns so that they can be hidden in the thickness of the walls. Because the beams are continuous, passing uninterrupted over the column lines, they benefit from the efficiency of continuity but without the extra fabrication cost associated with forming a full strength and rigid connection between discontinuous beams and continuous columns. The continuity of the beams across the the tops of the columns induces rotation at the top and bottom of the column under some loading arrangements resulting in curvature of the column, which may reduce the resistance of the column below that of an equivalent pin-ended strut, and therefore a design method for this form of construction is required. A method has been published [2] but this uses nominal moments and does not explicitly consider the magnitude of the slopes of the beams at the top and bottom of the column. This paper describes the development and validation of a new design method for square hollow section discontinuous columns which is safe, gives economical column sizes and is easy to apply by designers.

2.1 Braced frames with discontinuous columns

A typical frame using discontinuous columns is shown in Fig. 1 (much larger frames than that illustrated have been constructed, up to 14 storeys high). Each column piece is only one storey high and to provide a shallow construction depth, the floor, which may be composite construction using deep profile decking or pre-cast concrete, is supported on the bottom flange of asymmetric beams. Being built-in between the beams, the floor stabilises the beams (provided that precast units are fully grouted). This type of construction has a number of benefits including shallow floor construction [3,4] and reduced building height, beam continuity achieved with inexpensive connections [1], slender columns that can either be hidden in walls (or are of low visual impact if not hidden) and safe, easy crane hook access when lifting in pre-cast concrete floor units or metal decking because the columns do not extend above the floor beams until the next storey is erected. Set against these benefits are the disadvantages of: the greater number of individual column pieces to lift, so more crane time for column erection is required; continuous beams give fewer pieces but greater piece weights, possibly increasing the crane requirements; column piece labelling is critical wherever different wall

thicknesses of the same column sizes are used because all the columns appear to be identical but have different wall thicknesses; the design of the columns is problematic and guidance is required.

None of the design methods currently available are ideal for the design of discontinuous columns in braced frames. A new design method is required because (i) frame analysis with varying joint stiffness is too complex for routine design and (ii) methods based on nominal moments are uncertain and often give very conservative approximations. Research by Gent and Milner [5,6] and later by Davison et al. [7] and Gibbons et al. [8] demonstrated that the partial restraint inherent in nominally pinned columns is sufficient to increase the buckling resistance. (Readers interested in tracing the development of this work on 'moment shedding' are referred to Nethercot [9]). This earlier work suggested that it ought to be possible to devise a simple yet economic column design method for discontinuous columns. This paper details a study leading to the development of a proposed design method for square hollow section discontinuous columns in braced frames.
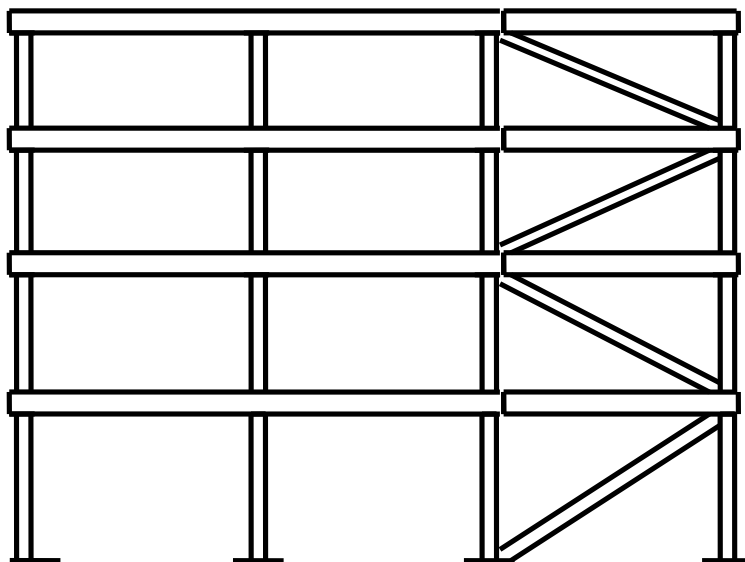
Fig. 1 Columns and beams in a typical frame with discontinuous column

2.2   A new column design approach required

When considering the behaviour of discontinuous columns two factors are of particular interest (1) the rotational stiffness of the column-beam joint (2) the effect of bending moments in the columns on the compression resistance. The axial compression in the columns in the upper stories of a building will be relatively small and if thin cap-plates are used, the connections will be flexible so the beam can rotate relative to the columns. This would result in higher sagging moments in the beams than would be calculated in a rigid frame analysis. In the lower stories of a building, the larger axial compression

clamps the columns and beams so that very little rotation of the beam relative to the column is possible, so the frame resembles a continuous one. Elastic analysis as a continuous frame requires the designer to either determine the stiffness of the joints accounting for the effect of axial compression or to specify cap-plates so thick that the joint is practically rigid even for low axial compression. The bending moments in the columns calculated by elastic analysis of a continuous frame can be of such a magnitude that they cause a significant reduction in the resistance to axial compression. Larger column sections are then required, increasing the bending stiffness further and attracting even more bending moment. This may lead to heavy columns, negating one of the attractions of the construction method i.e. to have small column cross-sections to allow them to be hidden in walls or limit the visual impact of exposed columns.

Modification of traditional design approaches, such as simple construction [10] where the columns are assumed to be pinned, or continuous construction [11] using elastic analysis of a rigid frame, are unsatisfactory. The former is potentially unsafe due to the effects of imposed end-rotations on the column which leads to reduced axial capacity; the latter requires heavy connections to realise the design assumptions and attracts too much moment to the columns which are desired to be kept small. A radically new approach is proposed in which the beams may be designed independently of the columns but the columns are designed taking account of the end rotation imposed on them by the slope of the beams.

The column design method exploits the moment-rotation relationship in beam-columns which (i) are subject to end-moments in the elastic domain but are not required to resist these end-moments to maintain static equilibrium of the structure and (ii) may be strained beyond the elastic limit.

Gent [5] and Gent and Milner [6] investigated the behaviour of columns under these conditions. Their test program applied moments to the end of the columns through a turnbuckle system (see Fig. 2(a)) in which the load relaxed as the end-rotation increased, thus the end-moment reduced as the curvature of the column increased. Initially the column was loaded by application of end rotations through the turnbuckle system. Next axial load was applied gradually up to failure of the column by buckling while the end-moments were measured. The end moments were seen to decrease as the axial compression increased, as shown in Fig. 2(b). This occured because the axial compression had to be resisted by the column to maintain static equilibrium whereas the end moment did not need to be resisted to maintain static equilibrium because increasing rotation of the column end allowed the turnbuckle system to relax and reduce the applied end-moment. Gent referred to this behaviour as "moment shedding". The phenomenon was also seen in large scale tests conducted by Davison et al. [7] and Gibbons et al. [8] and was incorporated in a proposed design method [12].
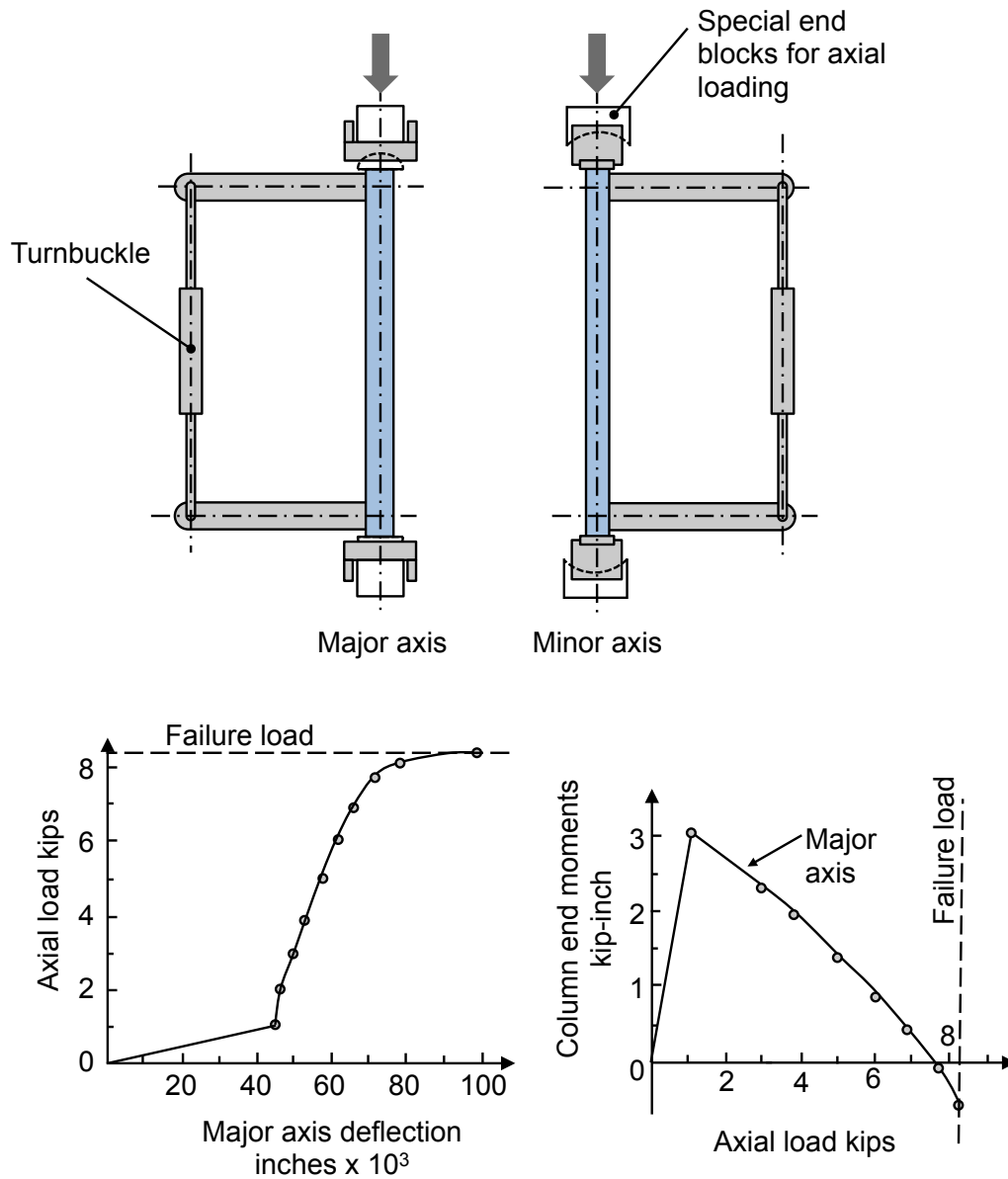
Fig. 2 Moment shedding from increasing axial load [6]

This behaviour is not what is commonly assumed in the design of beam columns. The common assumption is that the end-moments calculated by elastic analysis must always be resisted together with the axial load. In many cases this is appropriate, especially where the:

(a) beam size is chosen assuming a bending moment diagram that depends on moments in the columns;

(b) columns will fail by local buckling and/or lateral-torsional buckling if they are strained far beyond the elastic limit (likely in most I-section columns of common proportions, making the use of elastic analysis appropriate);

(c) columns form part of a sway-frame in which the columns must resist the moments to maintain static equilibrium with the applied horizontal loads.

However, in a braced frame if the beams are designed to carry the applied loads as if on knife-edge supports and the columns are not sensitive to failure by local or torsional buckling then the "moment shedding" behaviour observed by Gent and Milner can be used in the design process thus avoiding the need to estimate connection stiffness or analyse a frame to determine column end moments

3　Derivation of the proposed column design model

3.1　Developing a design model

To use the 'moment shedding' behaviour of the columns in a practical design method, it is necessary to develop a simple design model that incorporates the main aspects of the structural behaviour. The main features to be accounted for in modelling and designing discontinuous columns are the:

(a) End rotations of the columns. These are assumed to be equal to the slopes of the beams because the compression in the columns tends to clamp the beams and columns together. The slopes of the beams are calculated assuming that the beam is on knife-edge supports and the column stiffness is zero.

(b) Axial compression in the column.

(c) Bending resistance of the column as reduced by the coexistent axial compression.

Experimental studies [5-8] have demonstrated that columns shed the end moments caused by imposed end rotations if they are laterally and torsionally stable. This shedding of the end moments is not detrimental because the beams are designed to be able to carry the applied loads without assistance from bending moments in the columns.

The case of a column in single curvature is shown in Fig. 3(a). If the end moments are shed entirely, the bending moment in the column is that required to maintain equilibrium of the axial load in the deflected column. The bending moment diagram is shown in Fig. 3(b). The maximum moment in the column is equal to the product of the axial load and the maximum eccentricity from the straight line through the ends of the column. Provided that the column is in single curvature, the maximum eccentricity of the column lies within the triangle defined by the tangents to the column ends and the axis of the column before loading, as shown in Fig. 3(c). For equal and opposite end slopes, θ, the eccentricity at mid-height is less than $\theta h/2$. The end slopes, θ, are taken as the slopes of the beams calculated assuming that the beams are on knife-edge supports and derive no restraint from the columns.
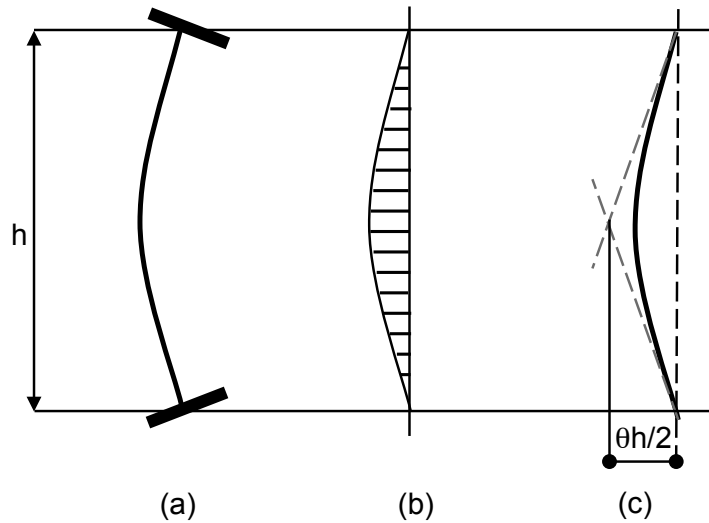
Fig. 3 Column in single curvature with no end moment (a) deflected column (b) bending moment induced by axial load (c) tangents to the column ends

Another case of a column in single curvature is shown in Fig. 4(a). This column has not shed all of the end moments induced by the slopes of the beams. Fig. 4(b) shows the bending moment diagram. If the end slopes of the column, θ, are the same as in Fig. 3, the actual deflection at mid-height is less for the column in Fig. 4 than for the column in Fig. 3. This is because the change of slope from end to end of the columns, 2θ, is the same but in Fig. 4 more of the curvature occurs at the ends which gives a smaller deflection at mid-height. Therefore, as was shown for the column in Fig. 3, the eccentricity at mid-height is less than θh/2.
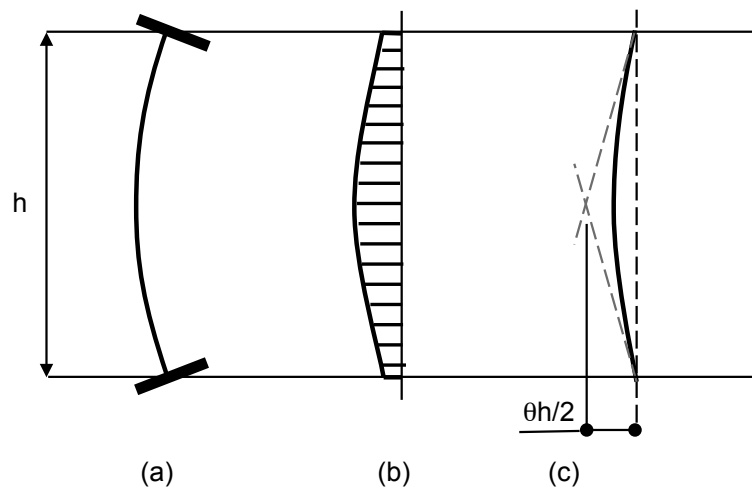
Fig. 4 Column in single curvature with end moments (a) deflected column (b) bending moment induced by axial load (c) tangents to the column ends

Fig. 5 shows two other cases for columns where the slopes of the beams are not equal and opposite. A column with equal end rotations ($\theta_1 = \theta_2$) is shown in Fig. 5(a). The bending moment diagram is shown in Fig. 5(b) assuming that moment shedding occurs. The projection of the end tangent to mid-height is shown in Fig. 5(c). A column with unequal end rotations, $\theta_1 > \theta_2$, is shown in Fig. 5(d). The bending moment diagram is shown in Fig. 5(e), assuming that moment shedding occurs only at the end with the maximum moment, and the projection to mid-height of the tangent to end with the greatest rotation is shown in Fig. 5(f).
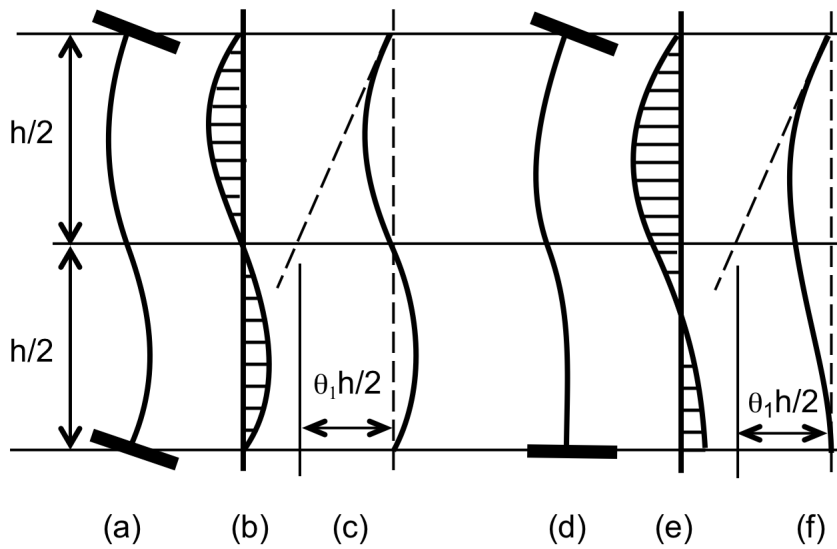
Fig. 5 Column in double curvature with unequal end-rotations: (a) beams applying equal rotations (b) moment induced by equal end rotations and load shedding (c) tangent at end with maximum end slope (d) beams applying unequal rotations (e) moment induced by unequal end rotations and load shedding (f) tangent at end with maximum end slope

In all the above cases, the resistance of the column to flexural buckling can be found by equating the destabilising effect to the stabilising effect. The stabilising effect is the reduced moment of resistance M_{Nr} of the column in the presence of axial compression, N_{Ed}. The destabilising effect is the moment applied to the column which is $N_{Ed}e$. Writing $e \leq \theta_1 h/2$, where θ_1 is the maximum end rotation, and equating the destabilising effect to the stabilising effect the column will be stable when:

$$N_{Ed}\theta_1 h/2 \leq M_{Nr} \tag{1}$$

In the case of a column with zero end-rotations, the axial resistance is limited to the strut buckling capacity, $N_{b,Rd}$. Equation (1) must therefore be modified to account for both initial geometric imperfections and residual stresses. Fig. 6(a) shows a typical column and Fig. 6(b) shows the bending

moment used in equation (1). Fig. 6(c) shows an additional moment of magnitude Ne_i to account for the effects of initial gometric imperfections and residual stresses.
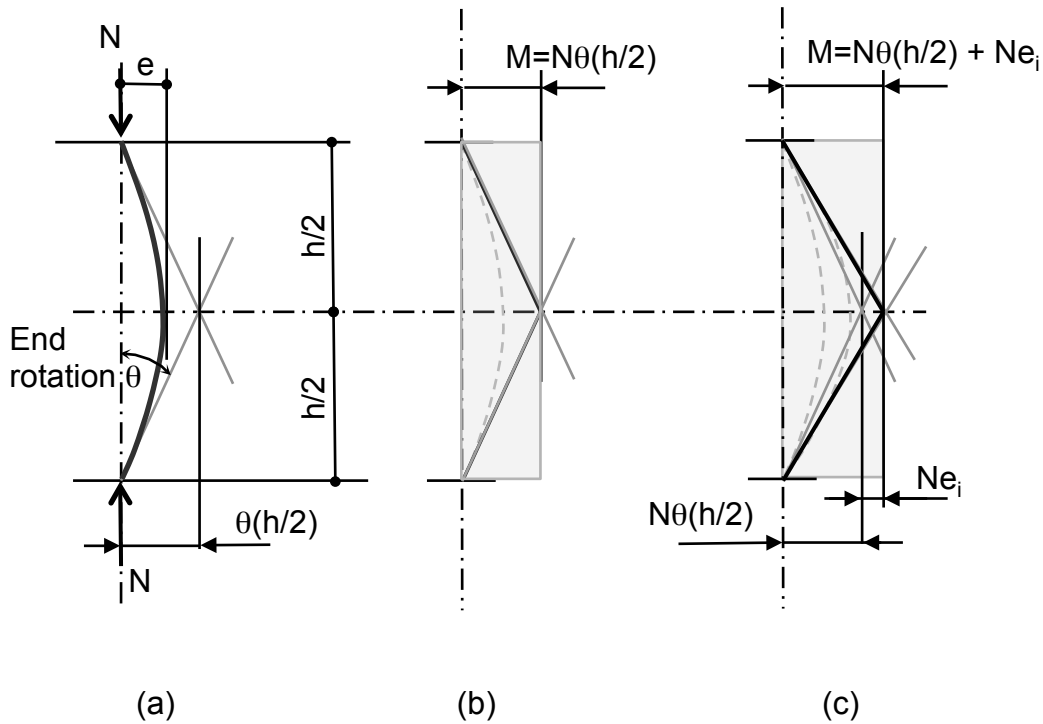
Fig. 6 Design model showing (a) column deflected by applied end rotations (b) bending moment induced by applied end rotations alone (c) design bending moment induced by applied end rotations plus design imperfection, e_i

When the effect of imperfections is included, the design equation (derived from moment equilibrium at mid-height) becomes:

$$N_{Ed} \times (\theta_{max} h/2 + e_i) \leq M_{Nr} \qquad\qquad (2)$$

where θ_{max} is the larger slope of the beams at the top or bottom of the column segment, e_i is the appropriate value of imperfection and M_{Nr} is the reduced moment of resistance of the column due to the coexistent axial compression, N_{Ed}.

3.2   Proposed design method

The proposed design method has two stages:

Stage1: Beam design

The beams are designed independently of the columns. Single span beams are designed as simply-supported beams and multiple-span beams are designed as beams on knife-edge supports. The beam slopes at the supports must be calculated for use in the column design. If the design is to BS 5950-1 [13] or to the ASCE manual [14], the designer should use "pattern loading" to find the worst loading condition for column buckling. However, if the design is to the Eurocodes and the structure is a

building, the designer would be free to ignore "pattern loading" according to the provisions of EN 1991-1-1 [15] Clause 6.2.2(1).

Stage 2: Column design

The columns are assumed to have no effect on the beam design and are designed to resist the design axial compression and satisfy the following criteria:

i. The rotation at each end of the column is equal to or greater than the rotation of the beam to which it is connected.

ii. The column must not rely on rotational restraint from the beams to maintain equilibrium.

The proposed column design model is shown in Fig. 6 and the equilibrium equation is derived from equation (2). The reduced moment of resistance of the column in the presence of axial load, M_{Nr}, is difficult to calculate accurately because the stress distribution is partially elastic and partially plastic as shown in Fig. 7(a). (There is additional complexity because residual stresses also affect the stress distribution.) However, as columns shed their end moments extensive plasticity is developed This means that the stress distribution at the critical cross section approaches that of the plastic moment of resistance reduced by axial load (see Fig. 7(b)), denoted in the Eurocode by the symbol $M_{N,Rd}$. The difference between the two stress distributions is shown diagramatically in Fig. 7(c). For the purpose of illustration a major difference is shown because Fig. 7(a) is the stress distribution in the case of a column with low curvature. For columns with high curvatures, the difference between the stress distributions for the M_{Nr} and $M_{N,Rd}$ would be much less.

(a) (b) (c)
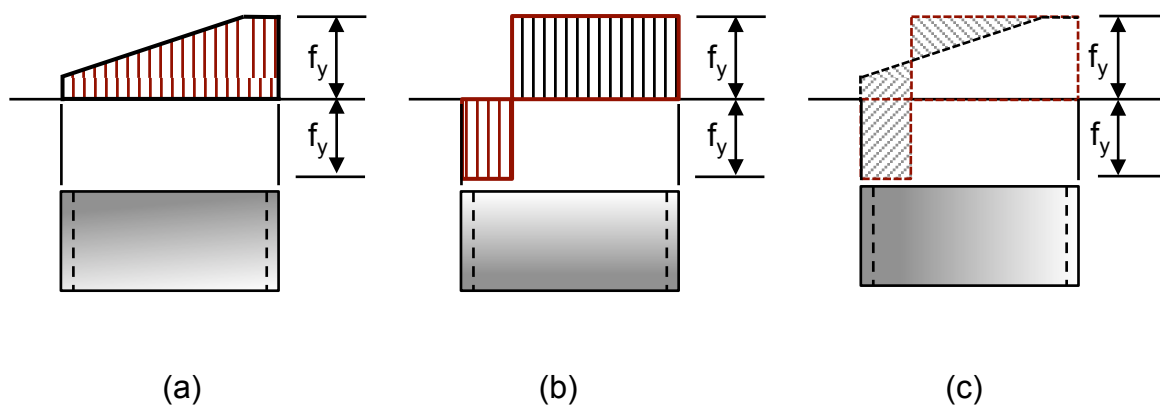
Fig. 7 Comparison of typical actual v plastic stress distributions for a column with low curvature (a) actual stress distribution assuming no residual stresses (b) plastic stress distribution (c) difference between (a) and (b)

Using $M_{N,Rd}$ is attractive because it is easy to define and easy to calulate but it is greater than M_{Nr}. One possibility is to define a factor F such that $M_{Nr} = FM_{N,Rd}$, where F is a factor less than or equal to 1.0 which accounts for the difference between M_{Nr} and $M_{N,Rd}$.

3.3 Defining the design value of the initial imperfection

To define the value of imperfection to be used, a value can be selected such that the column design model with θ_{max} as zero gives the same resistance as an appropriate national code for the pin ended strut case. Equation (2) thus becomes:

$$N_{Ed}(\theta_{max}h/2 + e_s) = FM_{N,Rd} \qquad (3)$$

where θ_{max} is the larger slope of the beams at the top or bottom of the column segment, e_s is the design value of the imperfection, $M_{N,Rd}$ is the design plastic moment resistance reduced due to axial force N_{Ed}, and F is a factor less than or equal to 1.0 which accounts for the difference between M_{Nr} and $M_{N,Rd}$. The approach is similar to classic second-order rigid-plastic analysis [16] except that the proposed design method includes the design imperfection.

In cases of low curvature, the difference between the actual stress distribution and the classic plastic stress distribution, as shown in Fig. 7(c), is significant. Where the beam above and the beam below a column have no rotation, the resistance of the column would be expected to be not less than the buckling resistance of a pin-ended strut. Therefore the additional imperfection in equation (3) must be such that the calculated resistance at zero applied end-rotation is equal to the strut resistance. This allows the new design method to be calibrated to whatever design code is specified by the calculation of an imperfection, e_s.

For a strut with a gross cross-sectional area, A, the imperfection, e_s, may be calculated as follows:

1. Calculate the buckling load of the column, N_b, as if it were a pin-ended strut using the specified design code.

2. Calculate the area, A_b, stressed to the design yield stress, f_{yd} , required to resist the pin-ended strut buckling load, N_b , i.e.

   $A_b = N_b / f_{yd}, \qquad (4)$

   where the design yield stress, f_{yd}, is the characteristic yield stress reduced by the appropriate material factor for cross-sectional resistance in the specified design code, for example using

   EN 1993-1-1, $\qquad\qquad f_{yd} = f_y/\gamma_{M0}, \qquad (5)$

BS 5950-1, $\qquad$ $f_{yd} = p_y$, $\qquad$ (6)

AISC 360, $\qquad$ $f_{yd} = \phi F_y$, $\qquad$ (7)

3. Calculate the reduced plastic moment of resistance, M_{pr}, assuming the area A_b is located around the centroid of the section and resists the axial load with the remaining part of the section resisting the moment.

4. Calculate the imperfection, e_s, at the buckling load N_b from the assumption that

$N_b \, e_s = M_{pr}$, $\qquad$ (8)

so $e_s = M_{pr} / N_b$. $\qquad$ (9)

This imperfection, e_s, is the appropriate value for e_i of Fig. 6(c) at zero end-rotation.

4   VALIDATION OF THE METHOD

4.1   Analysis method

In order to validate the proposed design method, parametric studies were undertaken with an FE model created using Abaqus finite element software [17] and calibrated against the results of laboratory tests conducted with full-size columns. Particular attention was paid to three aspects of the design method:

1. Demonstrating that the factor F in equation (3) can be safely taken equal to 1.0. This is to be expected because the simplified rectangular bending moment diagram in Fig. 6(c) over-estimates the bending moment *applied* to the column but the classic plastic stress diagram in Fig. 7(b) over-estimates the bending moment *resistance* of the column. The two over-estimates tend to compensate for one another.

2. Confirmation that the design value of the initial imperfection can be reliably taken as the strut imperfection, e_s.

3. For different levels of column end-rotation, establishing what breadth-to-thickness ratio is required to prevent plasticity causing local instability of the tube walls. This aspect is discussed in detail in King and Davison [19].

   Abaqus [17] was used to conduct geometric non-linear and material non-linear analyses. The model used shell elements with the nodes and the mid-thickness of the elements in the plane of the centre-line of the walls of the column. The ends of the model are connected to a "spider" of rigid-body elements, whose legs radiate to the point of intersection of the centre-line of the column and the plane of the end of the column. Most analyses were conducted using a model of the entire column although the effect of mesh refinement was checked by using a half-model that comprised a column cut longitudinally along the centre-line of two opposite sides [18].

The mesh of the finite element model is shown in Fig. 8. The same proportions of elements, along the length of the member, and the same number of elements were used for all full models, whatever the member length. The element mesh of the walls divides each wall into 6 elements across the width. The analyses assumed elastic/perfectly plastic material behaviour with the yield stress based on coupon test results [20]. The residual stress pattern was taken as shown in Fig. 9 with f_r assumed as 10% of the minimum specified yield stress, which is typical for a hot-finished hollow section.
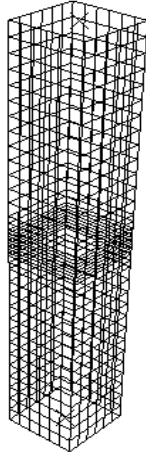
Fig. 8 Finite element model mesh of full model
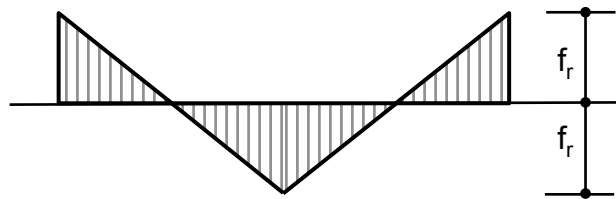
Fig. 9 Bi-triangular residual stress pattern (on all sides)

4.2   Comparison of analysis with test results

As the finite element model was to be used to confirm the structural behaviour assumed in the proposed design method and to conduct an extensive parametric study, it was first necessary to validate the model against a series of experimental tests reported in detail elsewhere [18,19]. A series of square hollow sections was tested in a hydraulic loading rig, see Fig. 10. All specimens were Celsius 355 120×120 Square Hollow Sections (SHS), hot-finished hollow sections produced by Tata Steel to EN 10210 in steel grade S355J2H. Table 1 presents details of the tests and comments on why each was conducted.

(b)

(a)   (c)

Fig. 10 Experimental set-up showing (a) Test rig with column in position (b) Shoe at bottom of
column (c) Sprung grip-frame to attach to LVDTs

Table 1

Test programme

Test No.	Specimen	
kc1	120 SHS × 5mm	pilot test
kc2	120 SHS × 5mm	pilot test continuation
kc3	120 SHS × 10mm	stable wall thickness
kc4	120 SHS × 10mm	stable wall thickness
kc5	120 SHS × 6.3mm	possible sensitivity to wall slenderness

kc6	120 SHS × 5mm wall	expect sensitivity to wall slenderness
kc7	120 SHS × 10mm wall	stable wall thickness
kc8	120 SHS × 10mm wall	stable wall thickness
kc9	120 SHS × 6.3mm wall	possible sensitivity to wall slenderness
kc10	120 SHS × 5mm wall	expect sensitivity to wall slenderness

The test specification required the columns to be installed into the rig with eccentricities such that the mid-height bending moment would be similar to that occurring in columns with the worst out-of-straightness allowed by current Standards. The test columns were found to be very nearly perfectly straight, so the columns were installed in the rig with equal eccentricity top and bottom of L/750 which is the value of out-of-straightness for a single storey column specified in BS EN 1090-2 [20].

The cross-sectional area of the model is slightly larger than the nominal area of the test specimen as the model uses the nominal wall thickness but assumes square corners whereas the test columns, being hot-finished sections, have curved corners with very tight external radii. The analysis results were multiplied by a reduction factor of 'nom/model', the ratio of the nominal area to model area, from Table 2 before making comparisons with the test results either by plotting or by calculations.

Table 2

Cross-sectional areas

Test No.	Wall thickness (mm)	Model area (mm^2)	Nominal area (mm^2)	nom/model
kc3, 4, 7, 8	10.0	4400	4290	0.975
kc5, 9	6.3	2865	2820	0.984
kc6, 10	5.0	2300	2270	0.987

A typical test plot is shown in Fig. 11. The maximum load reached is at B. Because the column was tested in a hydraulic testing machine it was possible to follow the unloading curve by skilful control of the oil pressure and flow rate. However, the rate at which the load on the specimen reduced was difficult to control and it was decided that it would be useful to stop the test and find a 'static' point – designated N_u, the point of unloadng – to remove any strain rate effects. Therefore at point C the pressure was backed off sufficiently to unload the specimen before reloading back up to point C where the column recommenced lateral deflection and end rotation up to failure.
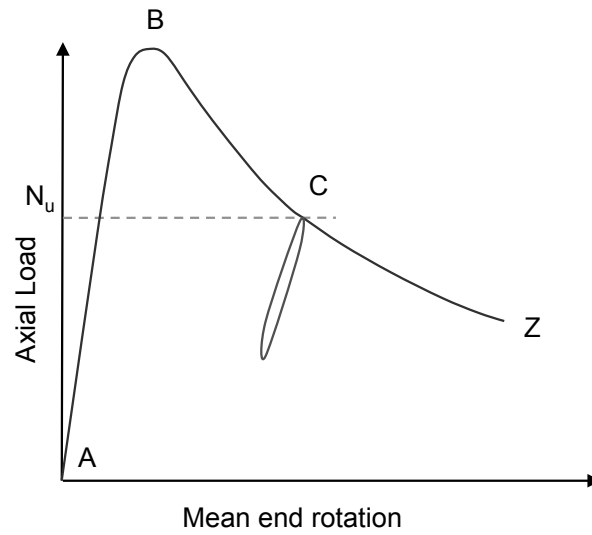
Fig. 11 Typical end-rotation v load from tests

The FE model was used to simulate the full-scale laboratory tests. For each test, the model was correlated to the test both by using the "yield" test coupon 0.2% proof stress as the yield stress in the elastic-perfectly plastic bi-linear material characteristic and by adjusting the initial imperfection in the model to reproduce the test behaviour of the test from zero to near maximum load (the "elastic" range of the test). As shown in Fig. 12, the FE analysis (shown as a dashed line) closely follows the test results (shown as a solid line).
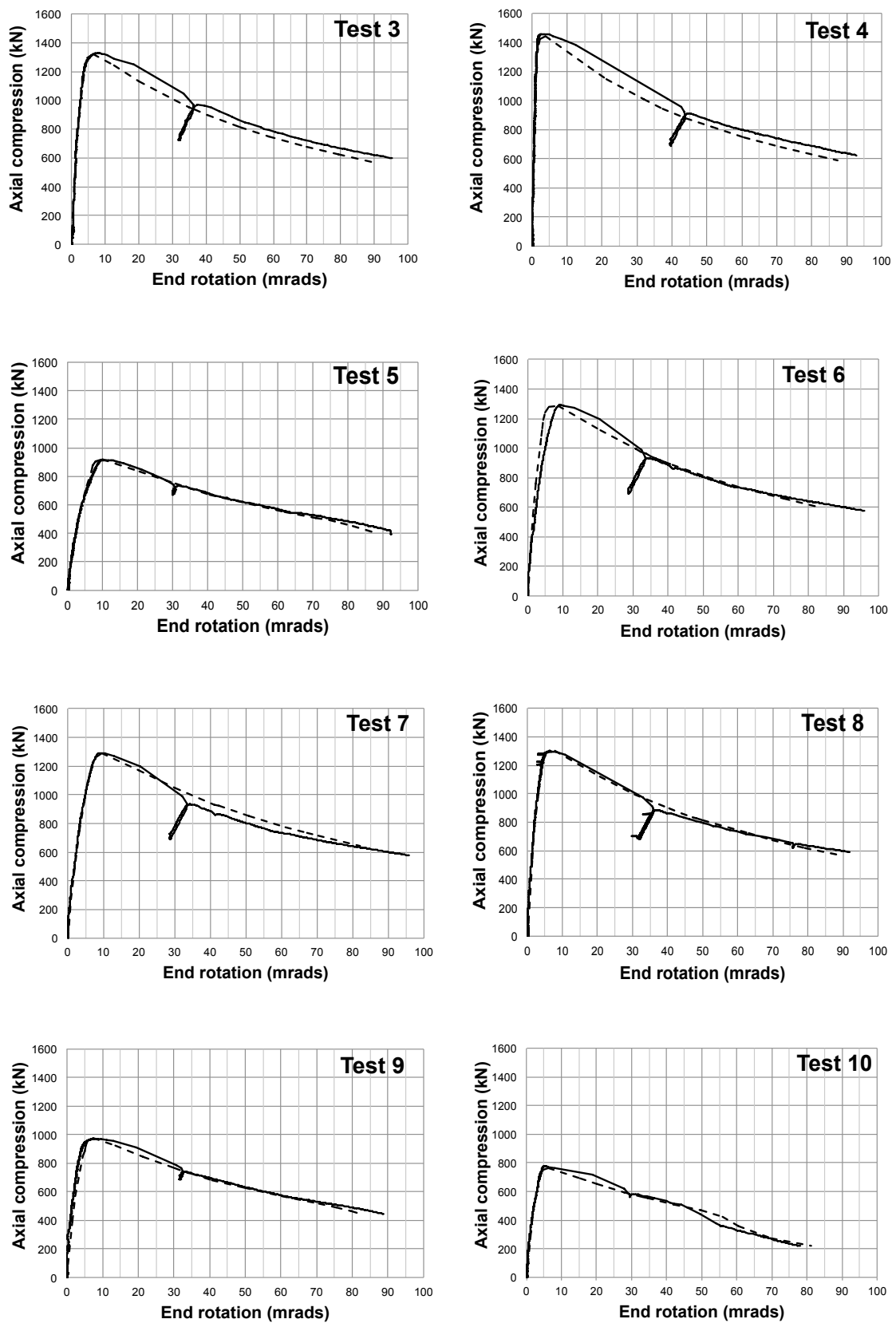
Fig. 12 Comparison of FE load against end rotation with experimental data

The relationship between the FE analysis and the test results is expressed as a correlation factor, c_f, on the end-rotations. The mean value of end-rotation in the laboratory tests at the point of unloading, designated θ_{Ct}, is shown in Fig. 13.
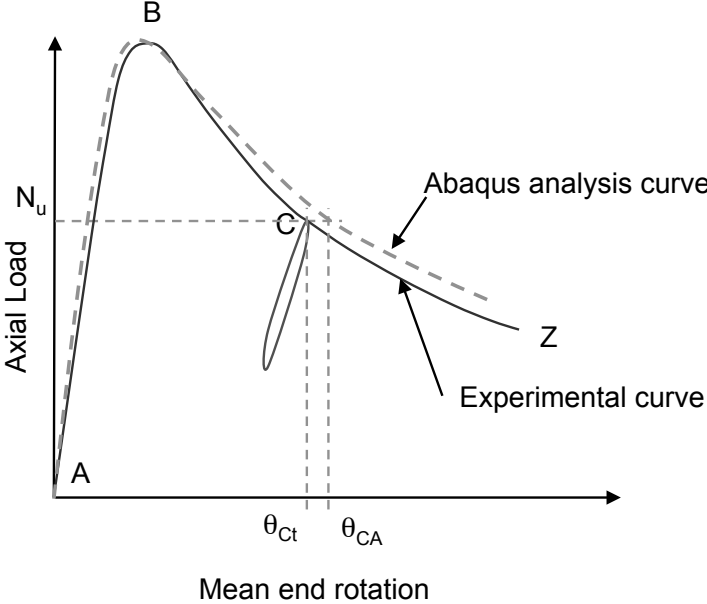
Fig. 13 Mean end-rotation v load: test v FE

The value of θ_{Ct} is found from the test results at the load N_u. The value of mean end-rotation predicted by FE, designated θ_{CA}, is found by interpolation to N_u from the adjacent points from the Abaqus output.

The correlation factor, c_f, is the ratio of the rotations,

$$c_f = \theta_{Ct} / \theta_{CA} \tag{11}$$

The values of c_f are given in Table 3. A residual stress, taken as 10% of the minimum specified yield (35.5MPa), was assumed in all cases in the distribution shown in Fig. 9.

Table 3

Comparison of analysis and test results

Test designation	kc3	kc4	kc5	kc6	kc7	kc8	kc9	kc10
Wall thickness (mm)	10	10	6.3	5	10	10	6.3	5
Maximum test load (kN)	1328	1458	915	695	1290	1298	971	777
0.2% proof stress (MPa)	375	390	428	389	see Note 1	375	431	402
Area factor (nominal/model area)	0.975	0.975	0.984	0.987	0.975	0.975	0.984	0.987
f_y used in analysis (MPa)	375	375	437	389	400	375	431	402
With equal eccentricity at the top and bottom of the analysis model								
Maximum analysis load (MPa)	1356	1481	930	703	1320	1333	991	773
Analysis load x area factor	1322	1444	915	694	1287	1300	975	763
% error	0.5	1	0	0.1	0.2	0.2	0.4	1.8
$e_t=e_b$	2.68	0.73	5.27	4.3	4.9	3.08	3.15	2.55
Correlation factor, c_f	1.003	1.021	0.831	see Note 2	0.804	0.841	0.941	0.918

Note 1: 0.2% proof stress not known

Note 2: No unloading cycle in test, so no point at which to calculate correlation

The correlation factors of end-rotation at a given axial load varied between 1.021 and 0.804, with an average of 0.913. Therefore, the value of correlation factor selected for the calibration of the design model was taken as 0.800, giving a small margin below the lowest value. While 0.800 might be considered disappointing as a correlation of end-rotations from a finite element analysis of a structure in which considerable elastic zones remain, it is considered acceptable for the falling branch of a compression member which has been almost completely plastified. The correlation between test and analysis looks much better when examined from the more common point of view of loads. The lowest correlation factor for end rotation (0.804) was found from test kc7. For this test an axial load of 927 kN was recorded at the "static" point (N_u) compared with 1011 kN predicted by the FEA model at the same rotation. This gives a ratio of 0.920, which is good for the falling branch in a test which plastified almost the entire cross-section over a considerable length of the column.

4.3 Effects of breadth to thickness ratios of wall

The test results demonstrated that current codes permit cross section slenderness in plastic sections which are likely to lead to premature buckling in structures using plastic (inelastic) design. King and Davison [19] discuss this at some length and design limits are proposed for square hollow sections relating the cross-section slenderness to column end rotations.

5 PARAMETRIC STUDIES

5.1 Introduction

The proposed design model was originally conceived for end-rotations in one of the two rectangular planes of the square hollow section column. However, in real structures columns may have end-rotations in both rectangular planes (although this is unlikely for the type of construction considered here where the continuity of beams over the columns is in one direction only). Therefore these cases were studied for 140×140×10 columns of length 3.0m because this is the most representative length of columns expected to be used in practice. The study used columns with single curvature because single curvature is assumed in the design model as it gives the lowest resistance for a given magnitude of end rotation. The study considered initial imperfections in two different planes, one in a rectangular plane and the other at 45° to the rectangular planes.

5.2 Column behaviour

The behaviour of a column with ane initial imperfection in a rectangular plane was studied first; the initial imperfection was in the plane of the Y-axis, in the positive direction, as shown in Fig. 14. Ten cases were analysed, with the end rotations in the five planes shown in Fig. 14 and listed in Table 4. In five of the ten cases, the end rotations were applied to cause deflections in the +X/+Y quadrant. In the other five cases, the end rotations were applied to cause deflections in the -X/-Y quadrant.
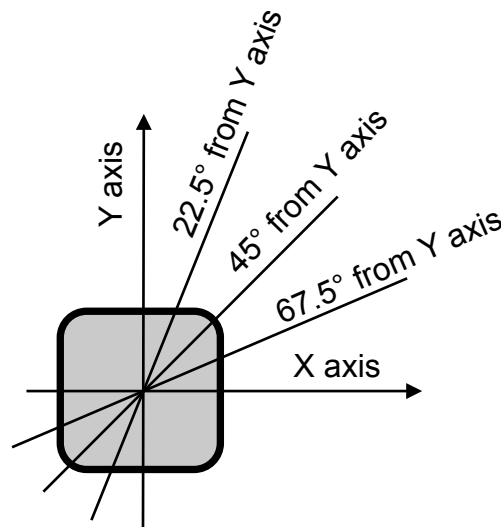
Fig. 14 Planes of rotation at 0°, 22.5°, 45°, 67.5° and 90° from the Y-axis.

The locus of a point at mid-height of the column is shown in Fig. 15. The origin of the graph is the initial position of the column at midheight (the initial imperfection was in the Y axis plane for all cases). As load is added to the columns it follows one of the paths indicated dependent upon the plane

in which the end rotation was applied. This shows that at lower levels of load, the point at mid-height deflects in the plane of the end-rotation but as the load approaches the maximum the point generally moves towards the plane of the initial imperfection i.e. X=0 plane (along the Y axis). The only exceptions are the columns with both (1) rotations moving the point away from the initial imperfection and (2) resultant end-rotations at less than 45° from the plane of the initial imperfection i.e. cases with θ = 225°; 202.5°. (These exceptions are not the governing cases for design because the initial imperfection reduces the eccentricity of the load at mid-height, so they have higher resistances than the other cases.)

Table 4

Planes of initial imperfections and end-rotations, see Fig. 15.

Plane of initial imperfection	Plane of end rotation
Y axis	Y axis
Y axis	X axis
Y axis	45° from Y axis
Y axis	22.5° from Y axis
Y axis	67.5° from Y axis
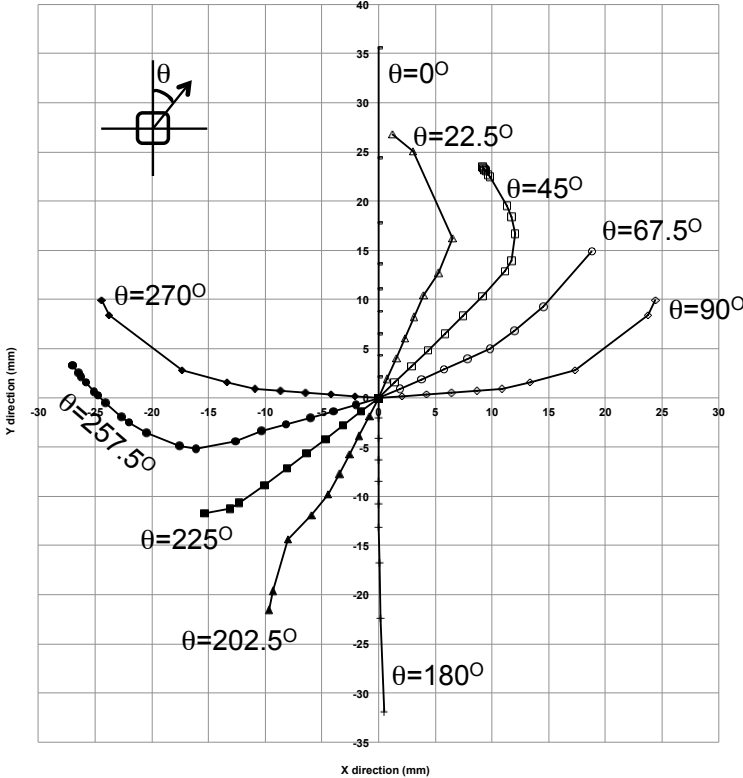
Fig. 15 Mid-height displacements –end-rotations applied at 0°, 22.5°, 45°, 67.5° and 90° from the Y axis with imperfection in plane of the Y axis

5.3   Development of the model for end-rotations in both rectangular planes

Fig. 15 shows that the point at the mid-height of the column follows path that does not remain in the same plane as the applied end-rotations as the column approaches failure. This means that the resistance in cases of end rotations in a plane at an angle to the rectangular axes cannot be accurately predicted by calculating the resistance of the cross-section to combined axial and bending in the plane of the applied rotations. It was therefore decided to test the design model for end-rotations in any plane by applying the true vector magnitude of end-rotation i.e. the root of the sum of the squares of the end-rotations in the two rectangular planes $\theta = \sqrt{(\theta_x^2 + \theta_y^2)}$ but calculating the resistance *assuming the end-rotations were in a rectangular plane*. This proved to give safe predictions of column resistance.

Table 5 summarises all the studies conducted and Fig. 16 presents the results (but for clarity only cases 1,2,3 are shown). Cases 1 and 2 were analysed for 140×140×10 SHS columns of 1.5m, 3.0m and 6.0m lengths. Case 3 has been analysed for 140×140×10 SHS columns of 3.0m and 1.5m length only because the similarity of behaviour in the Cases 1 and 2 show that the Case 3 will be similar for all lengths of columns. Cases 4, 5 and 6 were performed for the 3.0m columns only because (i) the analyses of Cases 1, 2 and 3 had shown the similarities between the behaviour of 1.5m, 3.0m and 6.0m lengths and (ii) the 3.0m length of 140×140×10 SHS columns is expected to be the most representative of the proportions of the majority of structures in which discontinuous columns are used. The proposed design model provides conservative predictions of the axial resistance in all cases.

Table 5

Planes of initial imperfections and end-rotations, see Fig. 15

Case	Plane of initial imperfection	Plane of end rotation	Column height (metres)		
			1.5	3.0	6.0
1	Y axis	Y axis	✓	✓	✓
2	Y axis	X axis	✓	✓	✓
3	Y axis	45° from Y axis	✓	✓	
4	Y axis	22.5° from Y axis		✓	
5	Y axis	67.5° from Y axis		✓	
6	45° from X axis	45° from Y axis		✓	
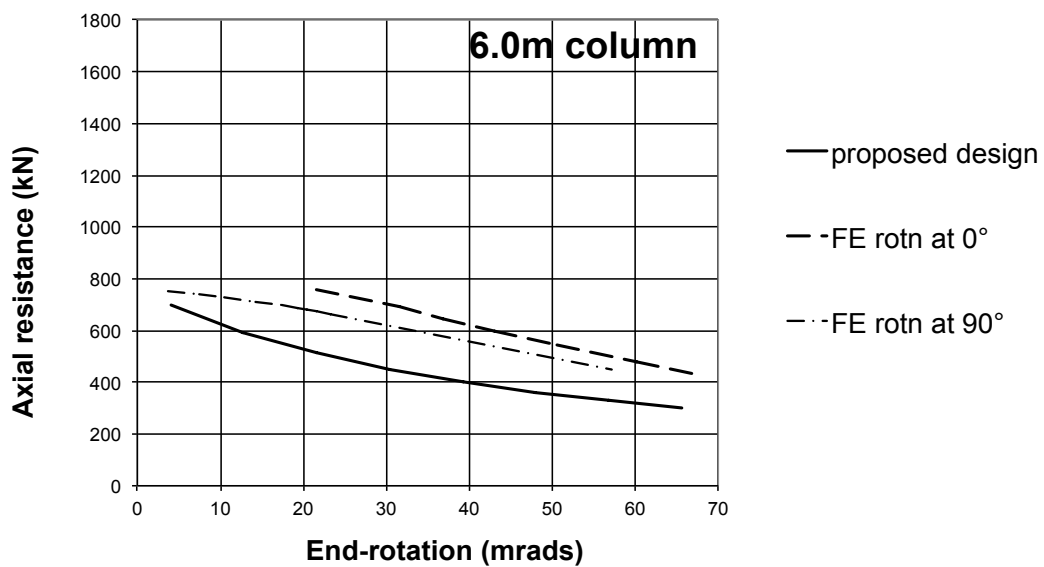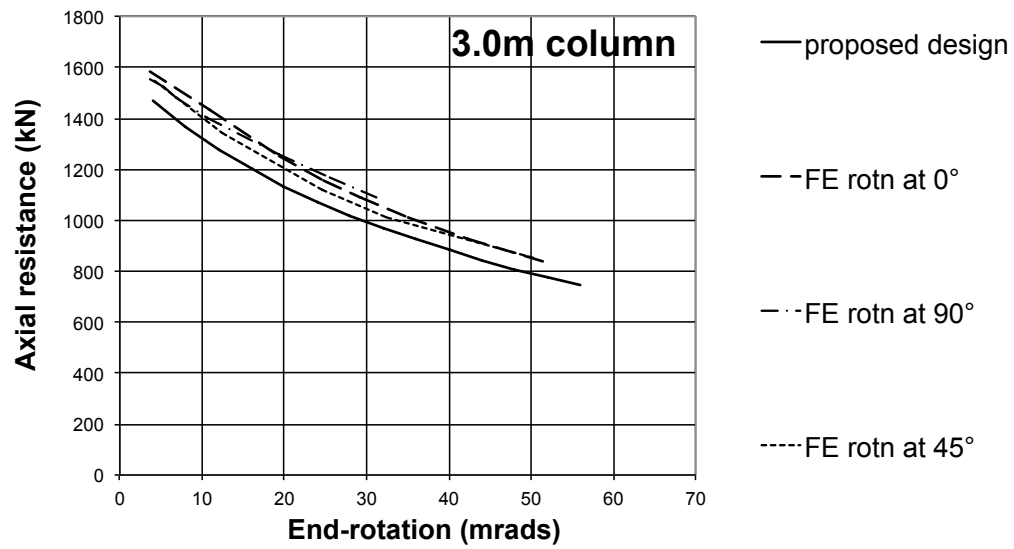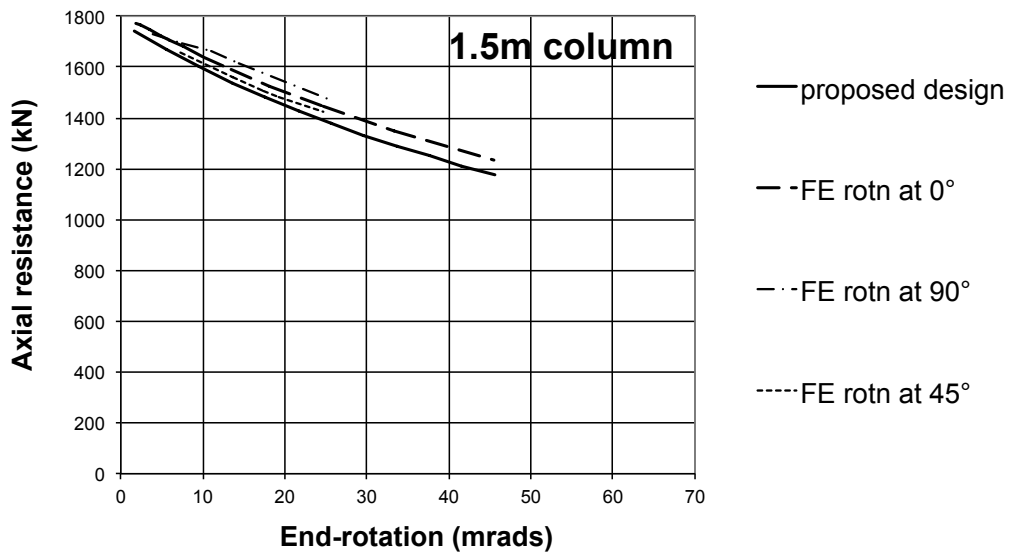
Fig. 16 Comparison of design model and FE load versus end-rotation

In summary, application of the model in all cases is as follows.

- The displacement at mid-height of the column caused by end rotations, as shown in Fig. 17(a), is calculated from the root of the sum of the squares of the end-rotations in the two rectangular planes. (In many cases the end rotation will be in a single plane.)

- The midheight displacement, $(h/2)\theta$, is applied in the calculation of the resistance as if it were in one of the rectangular planes. An appropriate value of imperfection, e_i, is added in the same rectangular plane thus the design displacement at midheight (see Fig. 17(b)) is calculated as:

$$e_d = (h/2)\theta + e_i \tag{12}$$

giving the design bending moment:

$$M_{Ed} = N_{Ed}e_d = N_{Ed}\{(h/2)\theta + e_i\} \tag{13}$$

where e_d is the design displacement along one rectangular axis of the SHS; θ is the greater end-rotation applied to the column at either end (or the root of the sum of the squares of the end-rotations in the two rectangular planes); e_i is the imperfection along a rectangular axis of the SHS. In the design model, e_i is taken as e_s which is the imperfection along a rectangular axis of the SHS such that the resistance to axial compression is equal to the pin-ended strut resistance as described in Section 3.6. The design bending moment, M_{Ed}, may then be compared with $M_{N,Rd}$, the design plastic moment resistance reduced due to axial force N_{Ed}.

(a)   (b)
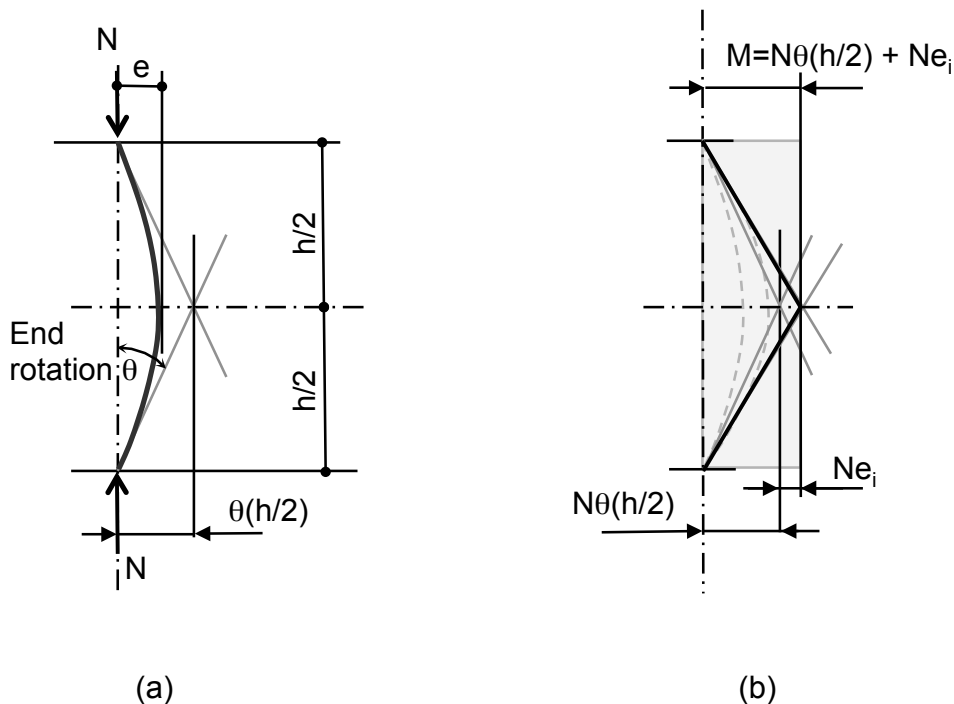
Fig. 17 (a) Load and shape diagram (b) Design bending moment diagram including N_{ei}

6 Reliability of the proposed design model

6.1 Introduction

A parametric study was conducted to show the reliability of the model as a design tool over a wide range of slenderness and end-rotations. A separate parametric study was also conducted to establish the design limits for the wall breadth to thickness ratio to avoid local buckling, as reported in [19].

The section chosen was 140×140×10 SHS in S355 steel, the commonest grade of steel used for structural hollow sections in Europe. The 10mm wall thickness in a 140×140 SHS is thick enough not to suffer significant deformations even at high plastic rotations. This section was chosen because it is one of the largest currently used in multi-storey buildings with discontinuous columns and the extent of plasticity caused by end-rotations is more pronounced in larger sections as the end-rotations in the elastic range are less.

The reliability of this model is shown by two methods:
(1) One is by comparing the resistance v end-rotation curves from Abaqus (modified by the calibration factor C_f) with the curves from the proposed design model.
(2) The other is a comparison of the proposed design model with the test results.

6.2 Comparison of curves of resistance v end-rotation

The 140×140×10 SHS was analysed for lengths of 3.0m, a representative length for typical residential construction, and also for lengths of 1.5m and 6.0m to give a wide range of slenderness. End rotations were applied as equal and opposite because that is both the worst design case and the design case assumed in the design model. The resistances from the design model were calculated using a total mid-height eccentricity = e_s + (h/2)θ where θ = c_f×Abaqus end-rotation with c_f = 0.8. (The Abaqus rotation was reduced by the correlation factor to correct the overestimate of rotation given by Abaqus when compared to the test results, as discussed in Section 3.2.) It can be seen from the plots in Fig. 19 that the design model always underestimates the resistance of the column at any applied end-rotation.

6.3 Comparison of proposed design resistance with experimental results

The reliability of the proposed design method was assessed by comparison with the laboratory tests of the 120 square hollow sections. The resistance was calculated for the end-rotation at the "static point" of the corresponding test using the yield stress measured for that test specimen. The nominal section

properties are used because the properties were not measured for each specimen. The results are presented in Table 6. The mean of [test resistance]/[proposed method] = 0.861 and the standard deviation = 0.043, so the difference between the mean of the proposed method and the mean of the test resistance is 3.22 standard deviations. This shows that the proposed method has a high level of safety.

The independence of the accuracy of the proposed method from the wall thickness of the member is shown in Table 6. The number of tests is small, but the table show N_{method}/N_{test} values that the reliability is similar for the wall thicknesses of 5mm, 6.3mm and 10mm. The wall thickness did not affect the reliability because none of the sections experienced significant wall deformations at the static point.

6.4   Summary of proposed design method

The development of the method has been outlined in some detail in order to explain the underlying principles of the approach. Depending on the code or standard being used, the details of the calculations will vary slightly but the basic procedure is summarised as follows:

Step 1: Calculate the slope of the beams at the column supports

Step 2: Use the greater of the beam slopes at the top or bottom of the column as the column end rotation, θ_{max}

Step 3: Calculate the buckling load, N_b, assuming the column to be a pin-ended strut

Step 4: Find the area of the cross-section, A_b, required to resist the buckling load N_b .i.e. $A_b = N_b/f_{yd}$

Step 5: Calculate reduced plastic moment of resistance, M_{pr}, in the presence of the buckling load N_b

Step 6: Find the imperfection, e_s, satisfying the equilibrium condition $M_{pr} = N_b e_s$

Step 7: Calculate the design deflection, e_d, at the column midheight: $e_d = \theta_{max}h/2 + e_i$ where $e_i = e_s$

Step 8: Check that equilbrium condition $N_{Ed}.e_d \leq M_{Nr}$ is satisfied, where M_{Nr} is the reduced plastic moment of resistance in the presence of the design axial load $N_{Ed}.$.

Table 6

Comparison of proposed design method with experimental results

Test	kc3	kc4	kc5	kc8	kc9	kc10	set
Size	all tests 120 square						
Thickness (mm)	10	10	6.3	10	6.3	5	
Yield (MPa)	375	390	428	375	431	402	
End rotation (millirads)	36.3	35.8	30.7	30.3	32.5	29.6	
Test load, N_{test} (kN)	940	892	707	874	729	567	
$N_{test}/N_{plastic}$	0.584	0.533	0.586	0.544	0.600	0.622	
N_{method} (kN)	774	804	605	810	605	471	
N_{method}/N_{test}	0.823	0.901	0.856	0.927	0.831	0.831	
mean							0.861
standard deviation, σ							0.043
coefficient of variation							0.050
mean + 3σ							0.990
mean + 3.22σ							1.000

7   Conclusions

This paper has described a research investigation to develop and verify a design method for discontinuous columns in braced frame construction. The use of discontinuous columns offers a number of practical advantages but presents a challenge to designers. This new approach calculates the resistance of the column with *imposed rotations* rather than moments at its ends. It is based on the phenomenon of moment shedding i.e. at failure the column is assumed to have zero moment at each end.

To validate the method an experimental test programme was conducted along with a parametric study using FE models. The results of the parametric study show that the design model illustrated in Fig. 17 is valid using the:

1. resistance properties about a rectangular axis,
2. an applied end-rotation (even when not in a rectangular axis)
3. an initial imperfection, e_i, defined as the imperfection about a rectangular axis that gives the buckling resistance of a pin-ended strut, e_s.

The design model has been compared with FE results across a range of practical sizes and found to give safe results. Designers should have little difficulty in using the method, which can be adapted for use with any modern limit state design code, as it has many similarities with the design of pinned columns with which they are familiar. Caution should be exercised in situations where the column size or length differs greatly from the practical cases considered.

REFERENCES

[1] AD281: The use of discontinuous columns in simple construction New Steel Construction, February 2005

[2] AD283: The use of discontinuous columns in simple construction (Part 2) New Steel Construction, March 2005

[3] AD285 Floor systems for simple construction using discontinuous columns and continuous beams, New Steel Construction, April 2005.

[4] AD292 The use of discontinuous columns and shallow deck composite slabs on floor beams, New Steel Construction, October 2005.

[5] Gent, AR. Elastic-plastic column stability and the design of no-sway frames, Proceedings of the Institution of Civil Engineers, 34, June 1966 p129-152

[6] Gent, AR and Milner, HR. The ultimate load capacity of elastically restrained H-columns under biaxial bending, Proceeedings of the Institution of Civil Engineers, 43, Decmeber 1968, p685-704

[7] Davison, JB, Kirby, PA and Nethercot, DA. Column Behaviour in PR Construction - Experimental Behaviour, *ASCE Journal of Structural Engineering*, Vol 113, No 9, September 1987, pp 2032-2050

[8] Gibbons, C, Nethercot, DA, Kirby, PA and Wang, YC. An appraisal of partially restrained column behaviour in non-sway steel frames, Proceedings Institution of Civil Engineers, Structures and Buildings, **99**, February 1993, pp.15-28

[9] Nethercot, DA. The importance of combining experimental and numerical study in advancing structural engineering understanding, Journal of Constructional Steel Research, 58, 2002, pp 1283-1296

[10] NCCI: Determination of moments on columns in simple construction, SN005a-EN-EU; 2005 Download available at http://www.steel-ncci.co.uk

[11] Davison, JB and Owens GW, Steel Designers' Manual, 7th Edition, Wiley-Blackwell, 2012

[12] Kirby, PA, Bitar, SS and Gibbons, C. Design of columns in non-sway semi-rigidly connected frames, Proceedings of the First World Conference on Constructional Steel Design, ed. Dowling, PJ et. al. Mexico, December 1992

[13] BS 5950-1:2000 Structural use of steelwork in building - Part 1: Code of practice for design - Rolled and welded sections British Standards Institution 2000

[14] Plastic Design in Steel; A Guide and Commentary ASCE - Manuals and Reports on Engineering Practice - No. 41 American Society of Civil Engineers, 1971

[15] EN 1991-1-1:2002 Eurocode 1, Actions on structures. General actions. Densities, self-weight, imposed loads for buildings. CEN (European Committee for Standardization), 2002

[16] Horne, MR, Elastic-plastic failure loads of plane frames Proceedings of the Royal Society, Vol A, Part 274, pp 343-64, 1963

[17] Abaqus, Dassault Systèmes Simulia (www.3ds.com)

[18] King, CM. Column Design for Axial Compression and End Rotation, PhD Thesis, University of Sheffield, June 2010

[19] King CM and Davison JB. Cross-section slenderness limits for columns with plastic rotations, Journal of Constructional Steel Research, 95, 2014, pp 162-171 doi:10.1016/j.jcsr.2013.11.019

[20] BS EN 1090-2:2008 Execution of steel structures and aluminium structures. Part 2: Technical requirements for the execution of steel structures. British Standards Institution.